

# Accreting White Dwarfs As Supersoft X-ray Sources

M. Kato<sup>1,\*</sup>

Keio University, Hiyoshi, Kouhoku-ku, Yokohama, 223-8521, Japan

Received 30 July 2009, accepted 11 Nov 2009

Published online later

**Key words** binaries: close – novae, cataclysmic variables – X-rays: binaries – white dwarfs – winds, outflows

I review various phenomena associated with mass-accreting white dwarfs (WDs) in the view of supersoft X-ray sources. When the mass-accretion rate is low ( $\dot{M}_{\text{acc}} < \text{a few } \times 10^{-7} M_{\odot} \text{yr}^{-1}$ ), hydrogen nuclear burning is unstable and nova outbursts occur. A nova is a transient supersoft X-ray source (SSS) in its later phase which timescale depends strongly on the WD mass. The X-ray turn on/off time is a good indicator of the WD mass. At an intermediate mass-accretion rate an accreting WD becomes a persistent SSS with steady hydrogen burning. For a higher mass-accretion rate, the WD undergoes “accretion wind evolution” in which the WD accretes matter from the equatorial plane and loses mass by optically thick winds from the other directions. Two SSS, namely RX J0513–69 and V Sge, are corresponding objects to this accretion wind evolution. We can specify mass increasing WDs from light-curve analysis based on the optically thick wind theory using multiwavelength observational data including optical, IR, and supersoft X-rays. Mass estimates of individual objects give important information for the binary evolution scenario of type Ia supernovae.

© 2006 WILEY-VCH Verlag GmbH & Co. KGaA, Weinheim

## 1 Introduction

Accreting white dwarfs (WDs) become transient, intermittent, and persistent supersoft X-ray sources (SSSs) depending on the mass-accretion rate. We find various phenomena for wide ranges of time-scales and wavelength. In this paper I will review when and how the supersoft X-rays emerge from the WDs. Section 2 briefly introduces the stability analysis of accreting WDs. Section 3 deals with low mass-accretion rates; WDs experience nova outbursts and become transient SSSs in the later phase. With intermediate accretion rate hydrogen burning is stable and the WDs become persistent SSSs, which is the subject of Section 4. In case of high mass-accretion rate, optically thick wind inevitably occurs from the WD surface (accretion wind). Section 5 introduces quasi-periodic SSSs as a related object to this regime.

## 2 Stability analysis of accreting WDs

Sienkiewicz (1980) examined thermal stability of steady-state models for accreting WDs of various mass. For low accretion rate, the envelope is thermally unstable which triggers a hydrogen shell flash, but for higher accretion rate, nuclear burning is stable. Nomoto et al. (2007) reexamined this stability using OPAL opacity and confirmed Sienkiewicz’ results. The stable and unstable regions are denoted in Figure 1. The unstable part represents WDs with thin envelope in which energy generation is mainly due to compressional heating, and stable region does WDs with nuclear burning at the bottom of an extended envelope.

\* Corresponding author: e-mail: mariko@educ.cc.keio.ac.jp

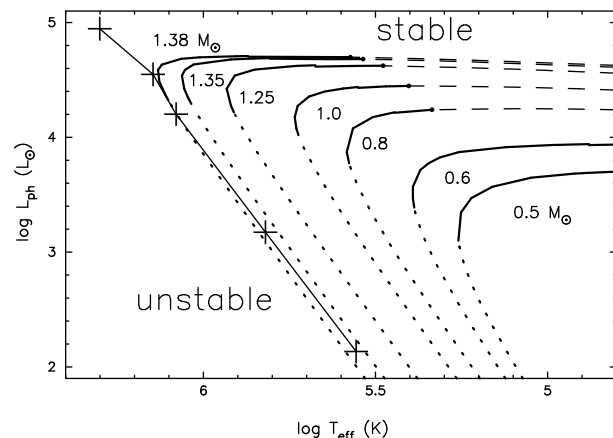


**Fig. 1** Loci of accreting WDs in the HR diagram. Each sequence corresponds to a mass of the WD which accretes matter of solar composition. The dotted part indicates unstable hydrogen burning, and solid and dashed parts stable burning. The dashed part is the region of optically thick wind mass loss in which supersoft X-ray flux cannot be expected due to the self absorption by the wind. “+” marks connected with a solid line denote “stable” solution claimed by Starrfield et al. (2004) for  $1.35 M_{\odot}$ .

These results on stability for steady-state models are consistent with evolutionary calculations of hydrogen-shell flashes on accreting WDs (e.g., Paczyński & Żytkow 1978; Sion et al. 1979; Prialnik & Kovetz 1995; Sparks, Starrfield & Truran 1978; Nariai, Nomoto & Sugimoto 1980; Townsley & Bildsten 2004) and also with static envelope analysis

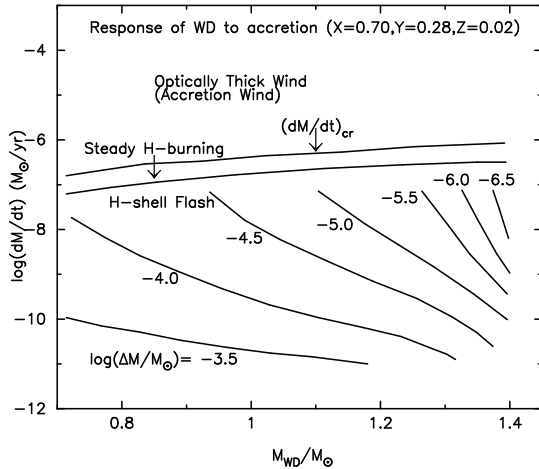


**Fig. 2** Response of WDs to mass accretion is illustrated in the WD mass and the mass-accretion rate plane. In the region above  $\dot{M}_{cr}$  strong optically thick winds blow. Hydrogen shell burning is stable for the region of  $\dot{M}_{acc} > \dot{M}_{std}$ . Steady hydrogen shell burning with no optically thick winds occur between the two horizontal lines, i.e.,  $\dot{M}_{std} \leq \dot{M}_{acc} \leq \dot{M}_{cr}$ . There is no steady state burning at  $\dot{M}_{acc} < \dot{M}_{std}$ , where unstable shell flash triggers nova outbursts. The ignition mass for shell flash is indicated beside the locus of the same ignition mass. See Hachisu and Kato (2001) for more detail.

(Iben 1982, and Sala & Hernanz 2005). Therefore, these results on stability of accreting WDs are considered as a kind of consensus among the researchers in this field.

It has to be noticed that Starrfield et al. (2004) presented different results for accreting WDs, that they call “surface hydrogen burning models”. In their calculation, WDs stably burn hydrogen for the accretion rates ranging from  $1.6 \times 10^{-9}$  to  $8.0 \times 10^{-7} M_{\odot} \text{yr}^{-1}$  and become type Ia supernovae. This result is in contradiction to our present understandings of stability of shell flash and all of the previous numerical results cited above. Nomoto et al. (2007) pointed out that these stable “surface hydrogen burning” is an artifact which arose from the lack of resolution in the envelope structure of Starrfield et al.’s models.

Figure 2 shows the response of the accreting WDs in the mass-accretion rate vs. WD mass diagram. The lower horizontal line denotes  $\dot{M}_{std}$ , the boundary between the stable and unstable regions of nuclear burning (i.e., the boundary of solid and dotted regions in Figure 1). If  $\dot{M}_{acc} < \dot{M}_{std}$ , hydrogen shell burning is unstable and nova outbursts occur. Otherwise, hydrogen burning is stable and no nova occurs.

The upper horizontal line in Figure 2 indicates  $\dot{M}_{cr}$ , the boundary that the optically thick winds occurs (i.e., the small circle at the left edge of the dashed line in Figure 1.) In the region above  $\dot{M}_{cr}$ , strong optically thick winds always blow (Kato and Hachisu 1994, 2009).

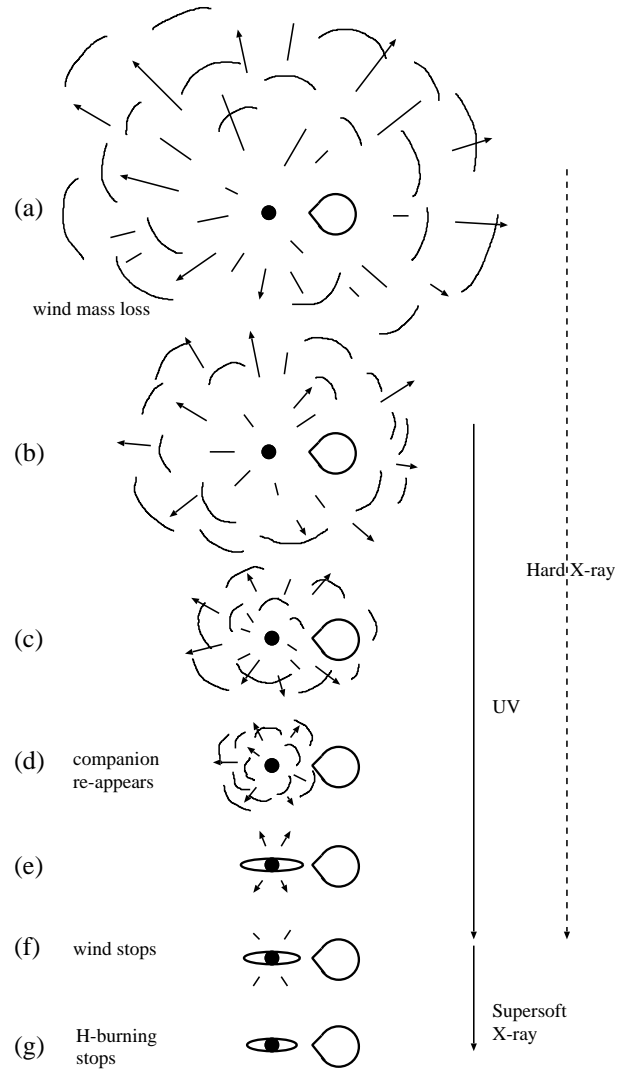


**Fig. 3** Evolution of nova outbursts. After the nova explosion sets in, the companion star is engulfed deep inside the photosphere (a); the photospheric radius moves inward with time due to strong mass loss. The companion emerges from the WD photosphere (d) and an accretion disk may appear or reestablish again (e). The optically thick wind stops (f). Hydrogen nuclear burning stops and the nova enters a cooling phase (g). The main emitting wavelength region shifts from optical to UV and then to supersoft X-rays. (taken Hachisu and Kato 2006)

In the intermediate accretion rate, i.e.,  $\dot{M}_{std} \leq \dot{M}_{acc} \leq \dot{M}_{cr}$ , the hydrogen burning is stable and no wind mass loss occurs. The WD burns hydrogen at the rate equal to mass accretion, and the WD keeps staying on the same position on the thick part in the HR diagram. The surface temperature is high enough to emit supersoft X-rays (see Figure 1). Therefore, this region corresponds to persistent X-ray sources.

### 3 Low mass-accretion rate

#### 3.1 Nova as transient SSSs

When the mass-accretion rate onto a WD is smaller than the critical value ( $\dot{M}_{\text{acc}} < \dot{M}_{\text{std}}$ ), unstable hydrogen shell flash triggers a nova outburst. The WD envelope quickly expands and it moves from the lower region (Fig. 1, dotted region) to the upper right region in the HR diagram.

Figure 3 shows the evolutionary change of nova binary during an outburst. After the nova outburst sets in, the envelope of the WD widely expands and strong wind mass loss begins. The optical photons dominate in the first stage which is replaced by the UV and then the X-ray photons as the photospheric temperature rises with time. The time scale of optical decline, UV and X-ray phases depends strongly on the WD mass and secondary on the chemical composition (e.g. Hachisu and Kato 2006). In general, a nova on a massive WD evolves fast so duration of the X-ray phase is also short, but for less massive WDs it lasts long. From the theoretical point of view, all novae become SSS in the later phase of the outburst, although the time scale is very different from nova to nova.

Supersoft X-rays are probably observed only after the optically thick wind stops, because supersoft X-rays are absorbed by the wind itself. Therefore, the X-ray turn on time and turn off time correspond to the epoch when the wind stops (f) and when hydrogen burning stops (g), respectively, in Figure 3.

Hard X-rays originate from internal shocks between ejecta (Friedjung 1987; Cassatella et al. 2004; Mukai and Ishida 2001) or between ejecta and the companion (Hachisu and Kato 2009b), therefore, it can be detected during the period as indicated by the dashed line in Figure 3.

#### 3.2 Light-curve fitting of classical nova

Nova light curves can be theoretically calculated using optically thick wind theory of nova outburst for a given set of WD mass and chemical composition of the envelope (Kato and Hachisu 1994). In general, novae evolve fast in massive WDs and slowly in less massive WDs, mainly due to the difference of ignition mass (less massive ignition mass in massive WDs). The optical and infrared (IR) fluxes can be basically well represented by free-free emission. There found a beautiful scaling law of optical and IR fluxes among a number of novae in different speed class, i.e., "universal decline law of classical nova" (Hachisu and Kato 2006). This property is useful to understand nova light curves that show a wide range of varieties. For example, we can extract a basic shape from a given light curve and recognize secondary shapes such as oscillatory behavior, multiple peaks, sudden optical drop associated to dust formation, and additional brightness due to emission lines in the nebula phase.

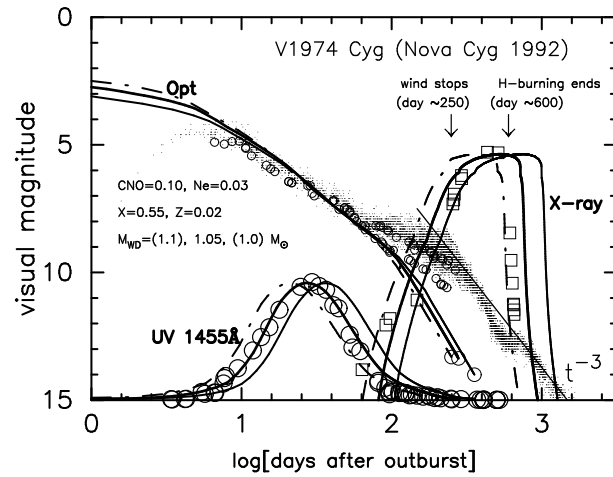


**Fig. 4** Light-curve fitting for V1974 Cyg. The supersoft X-ray data (open squares) as well as the UV 1455 Å (large open circles), visual (small dot) and  $V$ -magnitudes (small open circle) are shown. The lines denote theoretical curves for a chemical composition of  $X = 0.55$ ,  $X_{\text{CNO}} = 0.10$ ,  $X_{\text{Ne}} = 0.03$ , and  $Z = 0.02$ . The model of  $1.05 M_{\odot}$  WD (thick solid line) shows a best fitting to these observational data simultaneously. Two epochs, which are observationally suggested, are indicated by an arrow: when the optically thick wind stops and when the hydrogen shell-burning ends. (taken from Hachisu and Kato 2006)

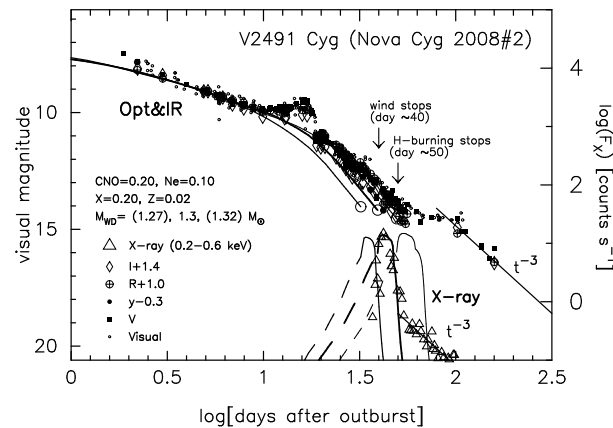


**Fig. 5** Light-curve fitting for V2491 Cyg. The upper bunch of data indicates optical and near-IR observational data, and the lower X-ray data. The best-fit theoretical model is a  $1.3 M_{\odot}$  (thick blue line) for the envelope chemical composition with  $X = 0.20$ ,  $Y = 0.48$ ,  $X_{\text{CNO}} = 0.20$ ,  $X_{\text{Ne}} = 0.10$ , and  $Z = 0.02$ . Supersoft X-rays are probably not detected during the wind phase (dashed part) because of self-absorption by the wind itself. The  $F_{\lambda} \propto t^{-3}$  law is added for the nebular phase. See Hachisu and Kato (2009a) for more detail.

Figure 4 shows an example of light-curve fitting. The lines marked “opt” represent calculated light curves. In the later phase the visual light curve deviates from the theoretical lines due to contribution of strong emission lines (see Hachisu and Kato 2006 for more detail).

The decline rate of optical flux and durations of UV and X-ray fluxes depend differently on the WD mass and composition, therefore, multiwavelength observation is important to determine these parameters. In this case, the above authors determined the WD mass to be about  $1.05 M_{\odot}$  for a set of chemical composition shown in the figure caption.

The second example of light-curve fitting is V2491 Cyg. This nova is a very fast nova of which supersoft X-ray phase lasts only 10 days. Figure 5 shows the best fit model, that reproduces simultaneously the light curves of visual, IR and X-ray, is  $\approx 1.3 M_{\odot}$  WD with the set of chemical composition given in the legend of the figure. This nova shows the secondary maximum about 15 days from the optical peak. Except this secondary maximum and the very later nebula phase the optical and IR light curves follow the universal decline law which is indicated by solid lines. (see Hachisu and Kato 2009a for the magnetic origin of the secondary maximum.)

### 3.3 X-ray turn on/off time and WD mass

Hachisu and Kato (2009b) presented light-curve analysis for more than ten novae in which supersoft X-rays are detected and determined the WD mass. For example,  $0.85 M_{\odot}$  for V2467 Cyg (CO nova),  $0.95 M_{\odot}$  for V458 Vul (CO nova),  $1.15 M_{\odot}$  for V4743 Sgr, and  $1.2 M_{\odot}$  for V597 Pup.

Kato, Hachisu and Cassatella (2009) suggested that Ne novae have a more massive WD than CO novae and the boundary of CO and Ne WDs is at  $\approx 1.0 M_{\odot}$  from their mass estimates for seven IUE novae. The mass estimates in X-ray nova (Hachisu and Kato 2009b) is consistent with the above boundary of  $\approx 1.0 M_{\odot}$  although the chemical composition is not known in some novae. Umeda et al. (1999) obtained that the lowest mass of an ONeMg WD is  $1.08 M_{\odot}$  from evolutionary calculation of intermediate stars in binary. This means that a WD is not eroded much, even though it had suffered many cycles of nova outbursts. This may provide interesting information for binary evolution scenarios and chemical evolution of galaxies.

### 3.4 Recurrent novae

Recurrent novae repeat outbursts every 10-80 years. The evolution of the outburst is very fast. As the heavy element enhancement is not detected, their WD mass is supposed to increase after each outburst. One of the interesting light curve properties is the presence of plateau phase. U Sco shows a plateau phase of 18 days (Hachisu et al. 2000) and RS Oph 60 days which are an indication of the irradiated disk (Hachisu et al. 2006). Hachisu, Kato and Luna (2007) showed that the turn off epoch of supersoft X-ray

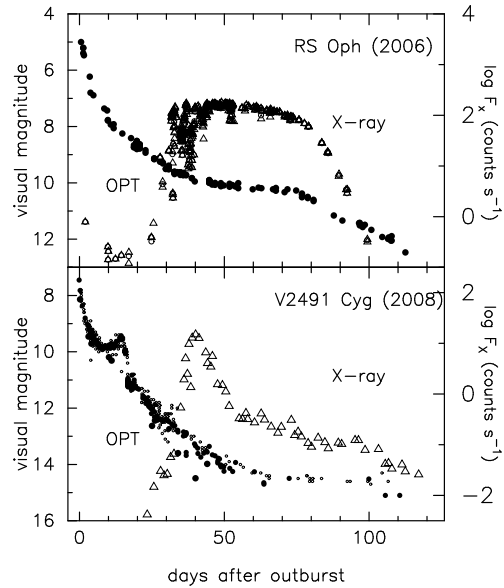


**Fig. 6** Comparison of light curves of RS Oph and V2491 Cyg. X-ray count rates and optical magnitudes are denoted by open triangles and filled circles, respectively. RS Oph data is taken from Hachisu et al. (2007), and V2491 Cyg data from Hachisu (2009a).

corresponds to the sharp drop immediately after the optical plateau phase (see Figure 6); They presented an idea that the long duration of the plateau in RS Oph is a result of additional heat flux from hot helium ash layer developed underneath the hydrogen burning zone. Therefore, the plateau is another evidence of increasing WD mass.

It is interesting to compare the visual and X-ray light curves of RS Oph with a classical nova V2491 Cyg. These objects show a similar rapid decline in the first optical phase except the secondary maximum of V2491 Cyg, and contain a very massive WD ( $1.35 M_{\odot}$  in RS Oph: Hachisu et al. 2007 and  $1.3 M_{\odot}$  in V2491 Cyg). However, RS Oph shows a long duration of supersoft X-ray phase, while V2491 does not.

This difference may be explained by the presence of a hot ash layer. In classical novae, hydrogen ignites somewhat below the WD surface due to diffusion during the long quiescent phase (Prialnik 1986), and ash produced in nuclear burning is carried upwards by convection and blown off in the winds. Then no helium layer develops underneath the burning zone. Heavy element enrichment observed in ejecta may support this hypothesis. On the other hand, in recurrent novae, diffusion process does not work in a short quiescent period, so hot helium ash can pile up and act as heat reservoir. This hypothesis needs to be examined more, perhaps in a next recurrent nova outburst.

## 4 Intermediate mass-accretion rate

In the intermediate mass-accretion rate ( $\dot{M}_{\text{std}} \leq \dot{M}_{\text{acc}} \leq \dot{M}_{\text{cr}}$ ), the hydrogen burning is stable and optically thick

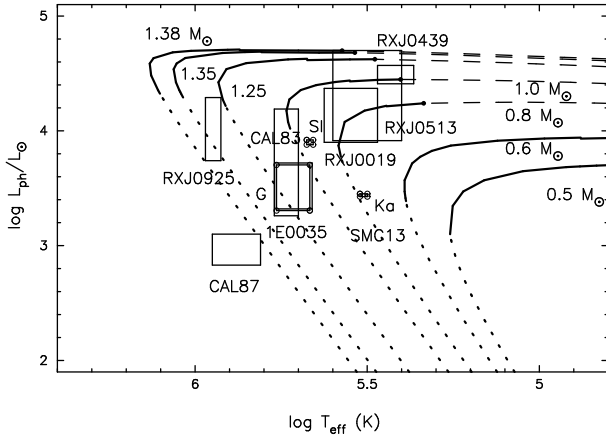


**Fig. 7** Same as Figure 1 but with SSSs (taken from Starrfield et al. 2004 except 1E0035). Three squares with small open circles denote SMC13 (G: Greiner (2000), SI: Suleimanov and Ibragimov (2003), K: Kahabka et al. (1999).

winds do not occur. The photospheric temperature of the WD is relatively high as indicated by solid lines in Figure 1. These WDs are observed as persistent SSSs.

#### 4.1 Steady hydrogen burning

van den Heuvel et al. (1992) interpolated supersoft X-ray sources as an accreting WD with high accretion rate ( $\approx 10^{-7} M_{\odot} \text{ yr}^{-1}$ ) so that it can undergo steady hydrogen nuclear burning. Figure 7 indicates the position of the SSSs in the HR diagram which are roughly consistent with theoretical steady burning phase (thick part), considering difficulties in determining observationally the temperature and luminosity.

#### 4.2 SMC13: a possible very slow nova?

It is to be noticed that some supersoft X-ray sources may be not exactly steady burning sources, but may be a remnant of nova outburst of very slow evolution. Kahabka and Ergma (1997) proposed an idea that the observational data of 1E0035.4-7230 (SMC13) can be explained in the framework of standard cataclysmic variable evolution of low mass WDs ( $\approx 0.6\text{-}0.7 M_{\odot}$ ).

Figure 8 demonstrates that a low mass WD ( $0.4 M_{\odot}$ ) undergoes nova outburst of extremely slow evolution. Its X-ray turn on/off times are 300 and 600 yrs, respectively for  $Z = 0.02$  and more slower for population II stars ( $Z = 0.004$  and  $0.001$ ). In these cases the supersoft X-ray phase starts when the optical magnitude drops by 6 mag, long after the optical peak. Therefore, we can detect no optical counterpart of a SSS nor find any record in literature.

Figure 7 also shows the estimated position of SMC13 by three squares with small open circles at each corner (two squares are very small). These positions are scattered among

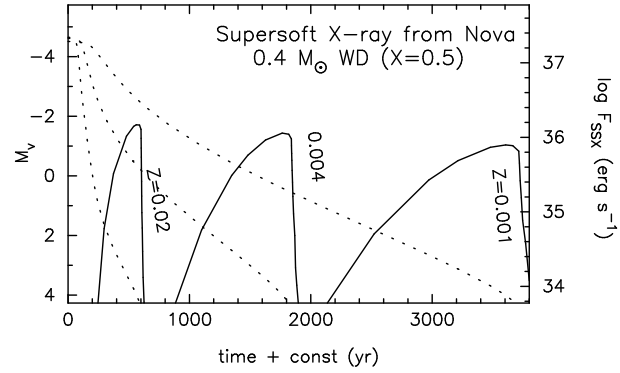


**Fig. 8** Theoretical light curves of visual and supersoft X-ray (0.1-0.6 keV) fluxes for  $0.4 M_{\odot}$  WD of various population ( $Z = 0.02, 0.004$  and  $0.001$ ).

authors with different method of analysis, but roughly consistent with solid part of the theoretical lines (a persistent source). If SMC13 is a very slow nova, its X-ray emission more than a decade suggests a less massive WD ( $< 0.6 M_{\odot}$ ) that has a smaller temperature. Thus, it is valuable to update the temperature and luminosity of SMC13 using unanalyzed high quality data recently obtained with satellites after BeppoSax and ROSAT.

## 5 High mass-accretion rate

### 5.1 Accretion wind

When the accretion rate is larger than  $\dot{M}_{\text{cr}}$ , the WDs cannot consume all of the accreted matter which is piled up to form an extended envelope. As the photospheric temperature decreases to reach the critical value (i.e., the rightmost point of the thick part in Figure 1), optically thick winds are accelerated due to Fe peak (at around  $\log T(\text{K}) \approx 5.2$ ) of the OPAL opacity (Kato and Hachisu 1994, 2009).

Hachisu and Kato (2001) proposed a binary system in which the WD accretes matter from the companion from the equatorial region and loses matter as a wind from the other regions as illustrated in Figure 9. They named such a configuration “accretion wind”.

In such a case, the WD burns hydrogen at the rate of  $\dot{M}_{\text{nuc}}$  and blows the rest of the accreted matter in the winds at the rate of about  $\dot{M}_{\text{acc}} - \dot{M}_{\text{nuc}}$ , where  $\dot{M}_{\text{nuc}}$  is the nuclear burning rate. Such a WD in this “accretion wind” corresponds to the dashed part in Figure 1.

This accretion wind is an important elementary process for binary evolution scenario to Type Ia supernova, because it governs the growth rate of the WD mass (e.g., Hachisu, Kato & Nomoto 1999a, Hachisu et al., 1999b, Han & Podsiadlowski 2006), as well as the mass-transfer rate from the companion which is regulated by stripping of companion surface by the wind (e.g., Hachisu, Kato & Nomoto 2008).

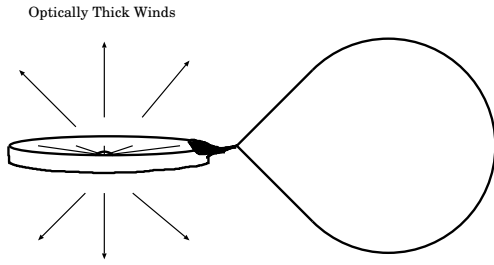


**Fig. 9** Optically thick winds blow from mass-accreting WDs when the mass-transfer rate from a lobe-filling companion exceeds a critical rate, i.e.,  $\dot{M}_{acc} > \dot{M}_{cr}$ . The white dwarf accretes mass from the equatorial region and at the same time blows winds from the polar regions.

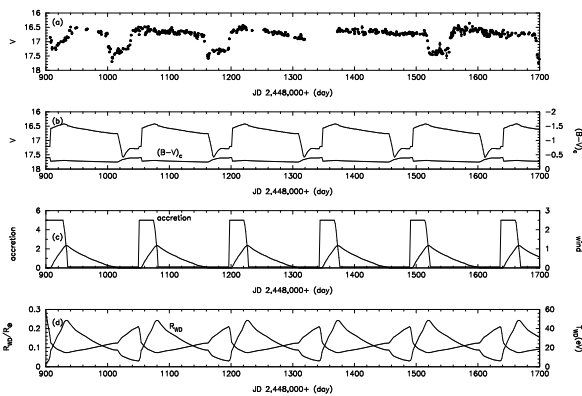


**Fig. 10** Self-sustained model of spontaneous winds for RX J05134–6951. (a) long term evolution of V magnitude. (b) model light curve of  $M_{WD} = 1.3 M_{\odot}$ . (c) change of accretion rate and wind mass-loss from WD envelope. (d) Change of WD radius and its temperature. (Taken from Hachisu and Kato 2003b.)

## 5.2 Accretion wind and SSS

There are two objects closely related to the accretion winds: RX J0513–69 and V Sge. Both of them are supersoft X-ray sources.

RX J0513–69 is an LMC SSS that shows quasi-regular transition between optical high and low states as shown in Figure 10 in which supersoft X-rays are detected only in the optical low states (Reinsch et al. 2000; Schaeidt, Hasinger, and Truemper 1993).

Hachisu and Kato (2003b) presented a transition mechanism between the high and low states. In the optical high state, the accretion rate is high enough and the photosphere expands to accelerate the winds (Figure 9). The WD locates in the low temperature region (dashed part in Figure 7) and no X-rays are expected. In the optical low state, mass-accretion rate is low and the photospheric temperature is enough high (in the solid part of Figure 7) to emit supersoft X-rays. No wind is accelerated. The above authors proposed a self-regulation transition mechanism that makes the binary back and forth between the optical high and low states.

When the mass-accretion rate is large, the WD is in the optical high state. The strong winds hit the companion and strip off a part of the companion surface. Thus the mass-transfer rate onto the WD reduces and finally stops, which causes the wind stop and the system goes into the optical low state. After a certain time, the companion recovers to fill the Roche lobe again and the mass transfer resumes, which causes wind mass loss. The resultant theoretical light curves depend on the WD mass and other parameters. The best fit model that reproduces the observed light curve best indicates the WD mass to be  $1.2 - 1.3 M_{\odot}$  (see Figure 10).

The second object is V Sge that also shows the similar semi-regular transition of light curve, although timescales are different. Its light curve is also reproduced by the transition model with the WD mass of  $1.2 - 1.3 M_{\odot}$  (Hachisu and Kato 2003a).

In these two systems the WD mass is increasing with time, because steady nuclear burning produces helium ash which accumulate on the WD. Therefore, they are candidates of type Ia supernova progenitor.

## References

- Cassatella, A., Lamers, H. J. G. L. M., Rossi, C., Altamore, A., González-Riestra, R.: 2004, *A&A* 420, 571  
 Friedjung, M.: 1987, *A&A* 180, 155  
 Greiner, J.: 2000, *NewA* 5, 137  
 Hachisu, I., Kato, M.: 2001, *ApJ* 558, 323  
 Hachisu, I., Kato, M.: 2003a, *ApJ* 590, 445  
 Hachisu, I., Kato, M.: 2003b, *ApJ* 598, 527  
 Hachisu, I., Kato, M.: 2006, *ApJS* 167, 59  
 Hachisu, I., Kato, M.: 2009a, *ApJ* 694, L103  
 Hachisu, I., Kato, M.: 2009b, *ApJ* submitted  
 Hachisu, I., Kato, M., Kato, T., Matsumoto, K.: 2000, *ApJ* 528, L97  
 Hachisu, I., Kato, M., Kiyota, S., et al.: 2006, *ApJ* 651, L141  
 Hachisu, I., Kato, M., Luna, G. J. M.: 2007, *ApJ* 659, L153  
 Hachisu, I., Kato, M., Nomoto, K.: 1999a, *ApJ* 522, 487  
 Hachisu, I., Kato, M., Nomoto, K.: 2008, *ApJ* 679, 1390  
 Hachisu, I., Kato, M., Nomoto, K., Umeda, H.: 1999b, *ApJ* 519, 314  
 Han, Z., Podsiadlowski, Ph.: 2006, *MNRAS* 368, 1095  
 Iben, I. Jr: 1982, *ApJ* 259, 244  
 Kahabka, P., Parmar, A. N., Hartmann, H. W.: 1999, *A&A* 346, 453  
 Kahabka, P., Ergma, E.: 1997, *A&A* 318, 108  
 Kato, M., Hachisu, I.: 1994, *ApJ* 437, 802  
 Kato, M., Hachisu, I.: 2009, *ApJ* 699, 1293  
 Kato, M., Hachisu, I., Cassatella, A.: 2009, *ApJ* submitted  
 Mukai, K., Ishida, M.: 2001, *ApJ* 551, 1024  
 Nariai, K., Nomoto, K., Sugimoto, D.: 1980, *PASJ* 32, 473  
 Nomoto, K., Saio, H., Kato, M., Hachisu, I.: 2007, *ApJ* 663, 1269  
 Paczyński, B., Żytkow, A.N.: 1978, *ApJ* 222, 604  
 Prialnik, D.: 1986, *ApJ* 310, 222  
 Prialnik, D., Kovetz, A.: 1995, *ApJ* 445, 789  
 Reinsch, K., van Teeseling, A., King, A. R., Beuermann, K.: 2000, *A&A* 354, L37  
 Sala, G., Hernanz, M.: 2005, *A&A* 439, 1061  
 Schaeidt, S., Hasinger, G., Trümper, J.: 1993, *A&A* 270, L9  
 Sion, E. M., Acierno, M. J., Tomczyk, S.: 1979, *ApJ* 230, 832  
 Sienkiewicz, R.: 1980, *A&A* 85, 295

- Sparks, W. M., Starrfield, S., Truran, J. W.: 1978, ApJ 220, 1063  
Starrfield, S., Timmes, F. X., Hix, W. R., Sion, E. M., Sparks, W.  
M., Dwyer, S. J.: 2004, ApJ 612, L53  
Suleimanov, V. F., Ibragimov, A. A.: 2003, ARep 47, 197  
Townsend, D.M., Bildsten, L.: 2004, ApJ 600, 390  
Umeda, H., Nomoto, K., Yamaoka, H., Wanajo, S. : 1999, ApJ  
513, 861  
van den Heuvel, E. P. J., Bhattacharya, D., Nomoto, K., Rappaport,  
S. A.: 1992, A&A 262, 97